Article

Magic Angle Spinning NMR Experiments for Structural Studies of Differentially Enriched Protein Interfaces and Protein Assemblies

Jun Yang, Maria Luisa Tasayco, and Tatyana Polenova

J. Am. Chem. Soc., **2008**, 130 (17), 5798-5807 • DOI: 10.1021/ja711304e • Publication Date (Web): 08 April 2008

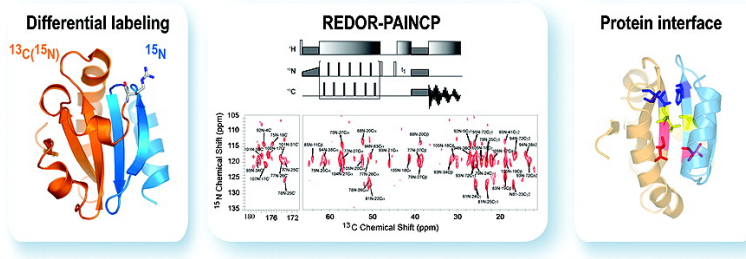

More About This Article

Additional resources and features associated with this article are available within the HTML version:

- Supporting Information
- Access to high resolution figures
- Links to articles and content related to this article
- Copyright permission to reproduce figures and/or text from this article

View the Full Text HTML

J|A|C|S
ARTICLES

Published on Web 04/08/2008

Magic Angle Spinning NMR Experiments for Structural Studies of Differentially Enriched Protein Interfaces and Protein Assemblies

Jun Yang,[†] Maria Luisa Tasayco,[‡] and Tatyana Polenova*[,†]

Department of Chemistry and Biochemistry, University of Delaware, Newark, Delaware 19716, and Department of Chemistry, The City College of New York, Convent Avenue at 138th Street, New York, New York 10031

Received December 27, 2007; E-mail: tpolenov@mail.chem.udel.edu

Abstract: Protein–protein interactions play vital roles in numerous biological processes. These interactions often result in formation of insoluble and noncrystalline protein assemblies. Solid-state NMR spectroscopy is rapidly emerging as a premier method for structural analysis of such systems. We introduce a family of two-dimensional magic angle spinning (MAS) NMR experiments for structural studies of differentially isotopically enriched protein assemblies. Using 1–73(^{13}C,^{15}N)/74–108(^{15}N) labeled thioredoxin reassembly, we demonstrate that dipolar dephasing followed by proton-assisted heteronuclear magnetization transfer yields long-range ^{15}N−^{13}C correlations arising exclusively from the interfaces formed by the pair of differentially enriched complementary fragments of thioredoxin. Incorporation of dipolar dephasing into the ^{15}N proton-driven spin diffusion and into the ^{1}H−^{15}N FSLG−HETCOR sequences permits ^{1}H and ^{15}N resonance assignments of the 74–108(^{15}N) enriched C-terminal fragment of thioredoxin alone. The differential isotopic labeling scheme and the NMR experiments demonstrated here allow for structural analysis of both the interface and each interacting protein. Isotope editing of the magnetization transfers results in spectral simplification, and therefore larger protein assemblies are expected to be amenable to these experiments.

Introduction

Protein–protein interactions result in formation of protein assemblies, such as microtubule-associated motor protein assemblies,[1] signaling protein assemblies,[2] and viral capsids and envelope assemblies.[3,4] Protein assemblies play vital roles in numerous biological processes and are also associated with various disease states.[5–7] In complex biological systems, such as amyloid fibrils, membrane proteins, viruses, biomaterials, and intact cells, many protein–protein interactions occur in noncrystalline and insoluble environments, and therefore solid-state nuclear magnetic resonance spectroscopy is arguably one of very few techniques that yield detailed structural information.[8] A number of recent reports demonstrate the potential of solid-state NMR methods for analysis of protein assemblies, such as bacteriophage viruses,[9] oligomeric membrane peptides and proteins,[10–13] amyloid fibrils,[14–20] and assemblies of soluble proteins.[21–23] With the recent developments in the uniformly enriched protein sample preparations for solid-state NMR,[22,24–26] hardware and pulse sequences for multidimensional correlations and determination of torsion angles[27–32] and distance constraints

[†] University of Delaware.
[‡] The City College of New York.

(1) Vale, R. D. *Cell* **2003**, *112*, 467–480.
(2) Yool, A. J. *Neuroscientist* **2007**, *13*, 470–485.
(3) Grunewald, K.; Cyrklaff, M. *Curr. Opin. Microbiol.* **2006**, *9*, 437–442.
(4) Klein, K. C.; Reed, J. C.; Lingappa, J. R. *AIDS Rev.* **2007**, *9*, 150–161.
(5) Verdier, Y.; Penke, B. *Curr. Signal Transduction Therapy* **2006**, *1*, 97–112.
(6) Lim, J.; Hao, T.; Shaw, C.; Patel, A. J.; Szabo, G.; Rual, J. F.; Fisk, C. J.; Li, N.; Smolyar, A.; Hill, D. E.; Barabasi, A. L.; Vidal, M.; Zoghbi, H. Y. *Cell* **2006**, *125*, 801–814.
(7) Hernandez, F.; Avila, J. *Cell. Mol. Life Sci.* **2007**, *64*, 2219–2233.
(8) Baldus, M. *Curr. Opin. Struct. Biol.* **2006**, *16*, 618–623.
(9) Goldbourt, A.; Gross, B. J.; Day, L. A.; McDermott, A. E. *J. Am. Chem. Soc.* **2007**, *129*, 2338–2344.
(10) Zheng, Z.; Yang, R.; Bodner, M. L.; Weliky, D. P. *Biochemistry* **2006**, *45*, 12960–12975.
(11) Hong, M. *J. Phys. Chem. B* **2007**, *111*, 10340–10351.
(12) Lange, A.; Giller, K.; Hornig, S.; Martin-Eauclaire, M. F.; Pongs, O.; Becker, S.; Baldus, M. *Nature* **2006**, *440*, 959–962.
(13) Porcelli, F.; Buck-Koehntop, B. A.; Thennarasu, S.; Ramamoorthy, A.; Veglia, G. *Biochemistry* **2006**, *45*, 5793–5799.
(14) van der Wel, P. C. A.; Lewandowski, J. R.; Griffin, R. G. *J. Am. Chem. Soc.* **2007**, *129*, 5117–5130.
(15) Shewmaker, F.; Wickner, R. B.; Tycko, R. *Proc. Natl. Acad. Sci. U.S.A.* **2006**, *103*, 19754–19759.
(16) Tycko, R. *Q. Rev. Biophys.* **2006**, *39*, 1–55.
(17) Chimon, S.; Ishii, Y. *J. Am. Chem. Soc.* **2005**, *127*, 13472–13473.
(18) Jaroniec, C. P.; MacPhee, C. E.; Bajaj, V. S.; McMahon, M. T.; Dobson, C. M.; Griffin, R. G. *Proc. Natl. Acad. Sci. U.S.A.* **2004**, *101*, 711–716.
(19) Petkova, A. T.; Buntkowsky, G.; Dyda, F.; Leapman, R. D.; Yau, W. M.; Tycko, R. *J. Mol. Biol.* **2004**, *335*, 247–260.
(20) Siemer, A. B.; Arnold, A. A.; Ritter, C.; Westfeld, T.; Ernst, M.; Riek, R.; Meier, B. H. *J. Am. Chem. Soc.* **2006**, *128*, 13224–13228.
(21) Etzkorn, M.; Böckmann, A.; Lange, A.; Baldus, M. *J. Am. Chem. Soc.* **2004**, *126*, 14746–14751.
(22) Marulanda, D.; Tasayco, M. L.; McDermott, A.; Cataldi, M.; Arriaran, V.; Polenova, T. *J. Am. Chem. Soc.* **2004**, *126*, 16608–16620.
(23) Yang, J.; Paramasivam, S.; Marulanda, D.; Cataldi, M.; Tasayco, M. L.; Polenova, T. *Magn. Reson. Chem.* **2007**, *45*, S73–S83.

10.1021/ja711304e CCC: $40.75

in uniformly and multiply labeled peptides and proteins,[33–36] complete or nearly complete resonance assignments have been accomplished in a number of globular proteins.[9,22,23,26,37–40] Complete three-dimensional structures have also been determined for several small proteins using solid-state NMR constraints.[41–44] However, to date detailed structural studies of uniformly or multiply isotopically labeled protein assemblies and of the intermolecular protein–protein interactions in such assemblies by solid-state NMR are scarce.[8,21–23]

In this report, we introduce a family of new two-dimensional magic angle spinning NMR experiments that permit structural analysis of the interfaces formed by the interacting proteins in the differentially (^{13}C,^{15}N/^{15}N) enriched protein assemblies. Several differential isotopic labeling strategies have been employed for solid-state NMR studies of protein–protein and protein−peptide complexes. One protocol involves incorporation of ^{13}C labels into a specific set of residues or an entire protein while ^{15}N labels are introduced into a different set of residues in the interacting protein partner. For instance, using ^{13}C and ^{15}N labeling of the different residues in gramicidin prepared in hydrated phospholipid bilayers,[45] both inter- and intramolecular distances have been measured with ^{13}C/^{15}N rotational echo double resonance (REDOR).[46] In another example, a ^{13}C labeled Crh protein monomer was mixed with an ^{15}N labeled Crh monomer, to yield the monomer–monomer interaction sites via

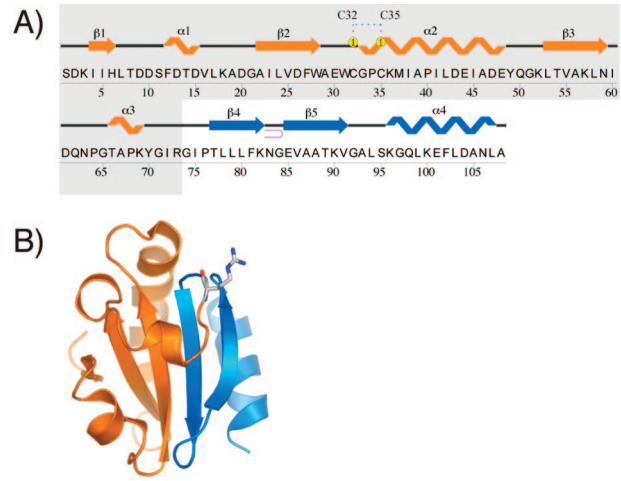

Figure 1. (A) Amino acid sequence and secondary structure of *E. coli* thioredoxin generated by PDBsum[67] from the X-ray coordinates deposited in the PDB file 2trx.ent.[68] The N-terminal portion of the protein (residues 1–73) is highlighted in orange; the C-terminal part (residues 74–108) is in blue. (B) Tertiary structure generated in Pymol.[69] The Arg-73 residue (the cleavage site for generating the complementary Trx fragments) is depicted in a stick representation. The complementary 1–73 and 74–108 fragments are shown in orange and blue, respectively.

the NHHC dipolar transfer experiments.[21] Another labeling protocol is to mix a uniformly (^{13}C, ^{15}N) enriched protein (or peptide) with its unlabeled interacting partner; this approach was applied to probe the ligand binding sites of a membrane protein.[47] Recently, we introduced a (^{13}C,^{15}N/^{15}N) labeling approach where a uniformly (^{13}C, ^{15}N)-enriched protein is complexed with its uniformly ^{15}N-enriched interacting protein partner.[22] Using this strategy in the 1–73(^{13}C,^{15}N)/74–108(^{15}N) and 1–73(^{15}N)/74–108(^{13}C,^{15}N) *E. coli* thioredoxin reassemblies, we reported resonance assignments, secondary structure, and medium- and long-range distance constraints for tertiary structure analysis of the (^{13}C,^{15}N) enriched individual fragments in each reassembly.[22,23] Thioredoxin reassembly is generated by proteolytic or chemical cleavage of *E. coli* thioredoxin at strategically designed positions, followed by purification of the complementary fragments and their subsequent reconstitution into a thermodynamically stable noncovalent complex.[48,49] Remarkably, the structure of the native thioredoxin is retained in the noncovalent reassembly as has been demonstrated by solution and solid-state NMR spectroscopy,[22,23,39,48–50] making the reassembled thioredoxin an excellent system for development of methods for structural analysis of proteins interfaces by NMR.

In this study, we employ 1–73(^{13}C,^{15}N)/74–108(^{15}N) thioredoxin reassembly (Figure 1) to establish MAS experiments that permit the identification of the residues forming the intermolecular interfaces and the resonance assignments of the ^{1}H and ^{15}N signals in the ^{15}N-enriched fragment. These experiments are based on heteronuclear ^{13}C/^{15}N or ^{13}C/^{1}H dipolar dephasing of the signals belonging to the residues from the ^{13}C,^{15}N-enriched portion of the reassembly followed or preceded by

(24) McDermott, A.; Polenova, T.; Bockmann, A.; Zilm, K. W.; Paulsen, E. K.; Martin, R. W.; Montelione, G. T. *J. Biomol. NMR* **2000**, *16*, 209–219.
(25) Martin, R. W.; Zilm, K. W. *J. Magn. Reson.* **2003**, *165*, 162–174.
(26) Pauli, J.; Baldus, M.; van Rossum, B.; de Groot, H.; Oschkinat, H. *ChemBioChem* **2001**, *2*, 272–281.
(27) Costa, P. R.; Gross, J. D.; Hong, M.; Griffin, R. G. *Chem. Phys. Lett.* **1997**, *280*, 95–103.
(28) Hong, M.; Gross, J. D.; Griffin, R. G. *J. Phys. Chem. B* **1997**, *101*, 5869–5874.
(29) Ishii, Y.; Terao, T.; Kainosho, M. *Chem. Phys. Lett.* **1996**, *256*, 133–140.
(30) Ladizhansky, V.; Veshtort, M.; Griffin, R. G. *J. Magn. Reson.* **2002**, *154*, 317–324.
(31) Chan, J. C. C.; Tycko, R. *J. Am. Chem. Soc.* **2003**, *125*, 11828–11829.
(32) Ladizhansky, V.; Jaroniec, C. P.; Diehl, A.; Oschkinat, H.; Griffin, R. G. *J. Am. Chem. Soc.* **2003**, *125*, 6827–6833.
(33) Jaroniec, C. P.; Tounge, B. A.; Herzfeld, J.; Griffin, R. G. *J. Am. Chem. Soc.* **2001**, *123*, 3507–3519.
(34) Jaroniec, C. P.; Filip, C.; Griffin, R. G. *J. Am. Chem. Soc.* **2002**, *124*, 10728–10742.
(35) Ramachandran, R.; Ladizhansky, V.; Bajaj, V. S.; Griffin, R. G. *J. Am. Chem. Soc.* **2003**, *125*, 15623–15629.
(36) Takegoshi, K.; Nakamura, S.; Terao, T. *Chem. Phys. Lett.* **2001**, *344*, 631–637.
(37) Igumenova, T. I.; McDermott, A. E.; Zilm, K. W.; Martin, R. W.; Paulson, E. K.; Wand, A. J. *J. Am. Chem. Soc.* **2004**, *126*, 6720–6727.
(38) Franks, W. T.; Zhou, D. H.; Wylie, B. J.; Money, B. G.; Graesser, D. T.; Frericks, H. L.; Sahota, G.; Rienstra, C. M. *J. Am. Chem. Soc.* **2005**, *127*, 12291–12305.
(39) Marulanda, D.; Tasayco, M. L.; Cataldi, M.; Arriaran, V.; Polenova, T. *J. Phys. Chem. B* **2005**, *109*, 18135–18145.
(40) Bockmann, A.; Lange, A.; Galinier, A.; Luca, S.; Giraud, N.; Juy, M.; Heise, H.; Montserret, R.; Penin, F.; Baldus, M. *J. Biomol. NMR* **2003**, *27*, 323–339.
(41) Lange, A.; Becker, S.; Seidel, K.; Giller, K.; Pongs, O.; Baldus, M. *Angew. Chem., Int. Ed.* **2005**, *44*, 2089–2092.
(42) Zech, S. G.; Wand, A. J.; McDermott, A. E. *J. Am. Chem. Soc.* **2005**, *127*, 8618–8626.
(43) Castellani, F.; van Rossum, B.; Diehl, A.; Schubert, M.; Rehbein, K.; Oschkinat, H. *Nature* **2002**, *420*, 98–102.
(44) Zhou, D. H.; Shea, J. J.; Niewkoop, A. J.; Franks, W. T.; Wylie, B. J.; Mullen, C.; Sandoz, D.; Rienstra, C. M. *Angew. Chem., Int. Ed.* **2007**, *46*, 8380–8383.
(45) Fu, R. Q.; Cotten, M.; Cross, T. A. *J. Biomol. NMR* **2000**, *16*, 261–268.
(46) Gullion, T.; Schaefer, J. *J. Magn. Reson.* **1989**, *81*, 196–200.
(47) Kiihne, S. R.; Creemers, A. F. L.; de Grip, W. J.; Bovee-Geurts, P. H. M.; Lugtenburg, J.; de Groot, H. J. M. *J. Am. Chem. Soc.* **2005**, *127*, 5734–5735.
(48) Chaffotte, A. F.; Li, J. H.; Georgescu, R. E.; Goldberg, M. E.; Tasayco, M. L. *Biochemistry* **1997**, *36*, 16040–16048.
(49) Tasayco, M. L.; Chao, K. *Proteins: Struct., Funct., Genet.* **1995**, *22*, 41–44.
(50) Yu, W. F.; Tung, C. S.; Wang, H.; Tasayco, M. L. *Protein Sci.* **2000**, *9*, 20–28.

either $^{15}N-^{13}C$ long-range magnetization transfer across the intermolecular interfaces or by $^{1}H-^{15}N$ or $^{15}N-^{15}N$ magnetization transfer within the ^{15}N-enriched fragment. The pulse sequences introduced in this work in conjunction with the homonuclear and heteronuclear correlation experiments employed in our previous studies of reassembled thioredoxin[22,23] constitute a general protocol for structural analysis of differentially (^{13}C,^{15}N/^{15}N) enriched protein assemblies by magic angle spinning NMR spectroscopy. The principal advantage of our approach is that it enables both the resonance assignments of the binding partners (and subsequently, their detailed structural characterization) and the structural analysis of the intermolecular interfaces. Additionally, the differential labeling and NMR experiments introduced here result in significant spectral simplification, and it is therefore envisioned that these protocols will be suitable for structural analysis of large protein assemblies.

Experiments and Methods

Sample Preparation. Overexpression and purification of U−^{13}C, ^{15}N isotopically enriched thioredoxin was described in previous reports.[22,48] Preparation of differentially enriched 1–73(U−^{13}C,^{15}N)/74–108(U−^{15}N) thioredoxin reassembly was reported in detail previously.[23] In brief, a proteolytic cleavage site was introduced at Arg-73. Each batch of ^{13}C,^{15}N- and ^{15}N- enriched purified thioredoxin was cleaved into two complementary fragments: one fragment encompassing the N-terminal residues 1–73, and the other, the C-terminal residues 74–108. The fragments were purified, and each fragment was reconstituted with its complementary partner containing complementary isotopic labels, for example, the 1–73(U−^{13}C,^{15}N) fragment was reconstituted with the 74–108(U−^{15}N) fragment. In Figure 1, the overall structure and the interface of the thioredoxin reassembled by reconstitution of 1–73/74–108 complementary fragments are shown. For solid-state NMR experiments, a sample of reassembled 1–73(U−^{13}C,^{15}N)/74–108(U−^{15}N) thioredoxin was prepared by controlled precipitation by slowly adding the solution of PEG-4000 containing 10 mM $NaCH_3COO$ and 1 mM NaN_3 (pH 3.5) to the solution of 70 mg/ml reassembled thioredoxin in 10 mM phosphate buffer (pH 7.0), as described previously.[22] The sample was centrifuged to remove the supernatant. Eleven mg of hydrated thioredoxin precipitate were packed into a 3.2 mm Varian rotor and sealed using an upper spacer and a top spinner.

Solid-State NMR Spectroscopy. NMR spectra were acquired on a 14.1 T narrow bore Varian InfinityPlus spectrometer operating at Larmor frequencies of 599.5 MHz for ^{1}H, 150.7 MHz for ^{13}C, and 60.7 MHz for ^{15}N. The 3.2 mm triple-resonance T3 MAS probe was employed. The MAS frequency in all experiments was 10.000 ± 0.001 kHz controlled by a Varian MAS controller. The temperature was calibrated for this probe at different MAS frequencies using a $PbNO_3$ temperature sensor,[51] and the actual temperature at the sample was maintained at −15 ± 0.5 °C throughout the experiments using the Varian temperature controller. ^{1}H, ^{13}C, and ^{15}N chemical shifts were referenced with respect to DSS, adamantane, and ammonium chloride used as external referencing standards.[52] For most of the experiments, the pulse lengths were 2.9 μs (^{1}H), 5 μs (^{13}C), and 5 μs (^{15}N). The $^{1}H-X$ (X = ^{15}N or ^{13}C) cross polarization employed a tangent amplitude ramp (80–100%); the ^{1}H radio-frequency field was 50 kHz; the center of the ramp on the heteronucleus was Hartmann–Hahn matched to the first spinning sideband. The contact times were 1.4 ms, and the Z-filter times were 20 ms in all experiments. During the rotational echo double resonance (REDOR) dephasing,[46] 100 kHz ^{1}H two pulse phase modulation (TPPM) decoupling[53] was employed, and the XY-8 phasing scheme[54] was applied to minimize the resonance offset of the rotor-synchronized π-pulse train. During the proton assisted insensitive nuclei cross polarization (PAINCP) transfers,[55] the radio-frequency field strengths on the ^{13}C and ^{15}N channels were 45 kHz, while the field strength on the ^{1}H channel was optimized for each experiment and was 57–63 kHz. In the $^{1}H-^{15}N$ heteronuclear correlation experiments, a flat CP with a short contact time of 170 μs was used. The $^{1}H-^{1}H$ homonuclear dipolar couplings were suppressed by frequency-switched Lee−Goldburg scheme (FSLG),[56] implemented by ramping the phase of the proton radiofrequency while keeping the proton carrier frequency unchanged. TPPI was used for frequency discrimination in the indirect dimension. Other acquisition and processing parameters are specified in the figure captions. Pulse sequence specific parameters are detailed in the section below.

Pulse Sequences. (Phase cycles for all sequences are presented in the Supporting Information.)

REDOR−PAINCP sequence is illustrated in Figure 2A. After an initial $^{1}H-^{15}N$ CP, a $^{13}C-^{15}N$ REDOR period is introduced to dephase the ^{15}N signals arising from the U−^{13}C,^{15}N-enriched fragment. The residual unwanted ^{13}C transverse magnetization excited by REDOR is removed by the ^{15}N Z-filter, after which only the ^{15}N magnetization of the ^{15}N-enriched fragment is retained. After the ^{15}N t_1 chemical shift evolution period, the ^{15}N magnetization is transferred across the interface to the ^{13}C,^{15}N-enriched fragment using the heteronuclear $^{15}N-^{13}C$ PAINCP transfer. The ^{13}C magnetization is finally detected during the t_2 period. As shown below, the final spectrum contains exclusively $^{15}N-^{13}C$ intermolecular through-interface correlations.

PDSD−REDOR sequence is illustrated in Figure 2B. After an initial $^{1}H-^{15}N$ CP followed by a ^{15}N t_1 chemical shift evolution period, a ^{15}N proton-driven spin diffusion (PDSD) mixing period is introduced to establish the sequential $^{15}N-^{15}N$ correlations. The subsequent $^{13}C-^{15}N$ REDOR dephasing period removes the ^{15}N signals arising from the U−^{13}C, ^{15}N-enriched fragment, followed by the ^{15}N *Z*-filter to eliminate the unwanted ^{13}C transverse magnetization excited by REDOR. The ^{15}N signals are finally detected during the t_2 period. As discussed below, the final spectrum contains sequential $^{15}N-^{15}N$ correlations arising exclusively from the U−^{15}N-enriched fragment.

HETCOR−REDOR sequence is illustrated in Figure 2C. The initial part of the sequence is the FSLG-based $^{1}H-^{15}N$ HETCOR experiment[57] employing a flat $^{1}H-^{15}N$ CP with a short contact time to establish one-bond $^{1}H-^{15}N$ correlations between the amide proton and nitrogen atoms in the entire protein, followed by the $^{13}C-^{15}N$ REDOR dephasing period to remove the ^{15}N signals arising from the U−^{13}C,^{15}N-enriched fragment. The ^{15}N *Z*-filter is employed to eliminate the unwanted ^{13}C transverse magnetization excited by REDOR, and the ^{15}N signals are finally detected during the t_2 period. As shown below, the final spectrum contains the $^{1}H-^{15}N$ correlations arising exclusively from the U−^{15}N-enriched fragment.

REDOR−HETCOR sequence is illustrated in Figure 2D. This two-dimensional experiment is a modification of a 1D ^{15}N-detected $^{13}C-^{1}H$ REDOR sequence reported by Schmidt-Rohr and Hong.[58] The ^{1}H magnetization evolves under the influence of the recoupled $^{13}C-^{1}H$ dipolar coupling using the REDOR filter, while the FSLG

(51) Neue, G.; Dybowski, C. *Solid State Nucl. Magn. Reson.* **1997**, *7*, 333–336.
(52) Morcombe, C. R.; Zilm, K. W. *J. Magn. Reson.* **2003**, *162*, 479–486.
(53) Bennett, A. E.; Rienstra, C. M.; Auger, M.; Lakshmi, K. V.; Griffin, R. G. *J. Chem. Phys.* **1995**, *103*, 6951–6958.
(54) Gullion, T.; Baker, D. B.; Conradi, M. S. *J. Magn. Reson.* **1990**, *89*, 479–484.
(55) Lewandowski, J. R.; De Paepe, G.; Griffin, R. G. *J. Am. Chem. Soc.* **2007**, *129*, 728–729.
(56) Bielecki, A.; Kolbert, A. C.; Levitt, M. H. *Chem. Phys. Lett.* **1989**, *155*, 341–346.
(57) vanRossum, B. J.; Forster, H.; deGroot, H. J. M. *J. Magn. Reson.* **1997**, *124*, 516–519.
(58) Schmidt-Rohr, K.; Hong, M. *J. Am. Chem. Soc.* **2003**, *125*, 5648–5649.

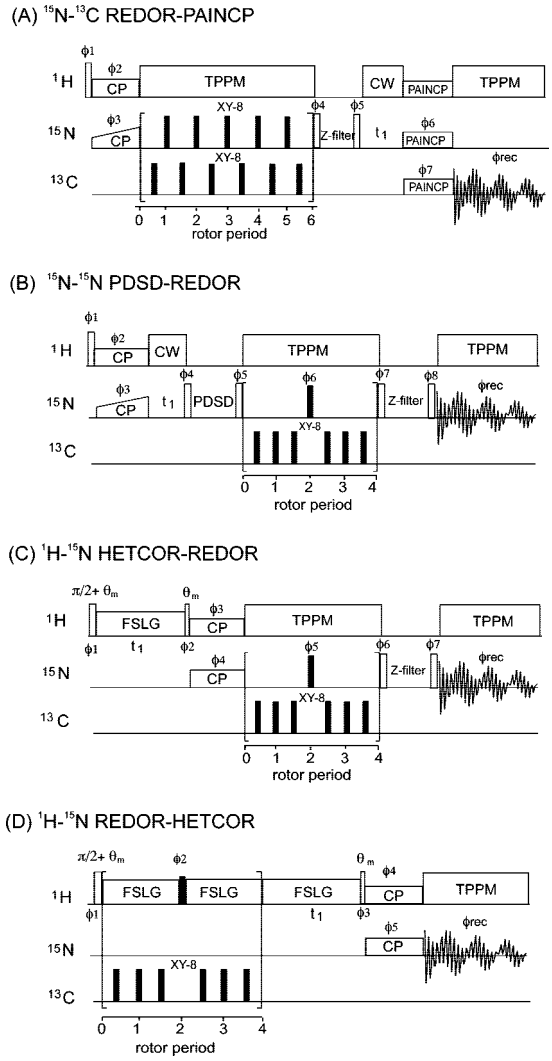

Figure 2. Pulse sequences for 2D ^{15}N−^{13}C REDOR−PAINCP (a), ^{15}N−^{15}N PDSD−REDOR (b), ^{1}H−^{15}N HETCOR−REDOR (c), and ^{1}H−^{15}N REDOR−HETCOR (d) used in this study. Open rectangles represent $\pi/2$ pulses (except where specified otherwise); filled rectangles represent π pulses. In the HETCOR−REDOR and REDOR−HETCOR experiments, θ_m represents the magic angle (54.7°) pulse. *XY*-8 phasing scheme was used in the rotor-synchronous REDOR π-pulse train. The complete phase cycles are given in the Supporting Information.

element is applied to suppress the ^{1}H−^{1}H dipolar interaction. Following the t_1 evolution under FSLG for the ^{1}H homonuclear decoupling, the ^{1}H magnetization is transferred to ^{15}N by a flat CP with a short contact time. The ^{15}N signal is finally detected during the t_2 period. As shown below, the final spectrum contains the ^{1}H−^{15}N correlations arising from the residues of the U−^{15}N-enriched fragment, whereas the cross peaks from the residues constituting the intermolecular interface show reduced intensity because of their partial $^{1}H^{N}/^{13}$C REDOR dephasing by the ^{13}C spins in U−^{13}C, ^{15}N-enriched fragment. As discussed below, both experiments produce ^{1}H/^{15}N correlations of the backbone amide NH groups with total elimination of signals from the doubly labeled fragment. The HN REDOR-HETCOR experiment results in additional intensity reduction of the residues close to the interface because of their $^{1}H^{N}/^{13}$C REDOR dephasing by the ^{13}C spins in the U−^{13}C, ^{15}N-enriched fragment. Similar ^{15}N/^{13}C REDOR dephasing is too weak to cause noticeable signal reduction in the HETCOR−REDOR experiment.

Data Processing and Analysis. All spectra were processed in NMRpipe[59] and analyzed in Sparky.[60] A 90°- or 60°-shifted sine bell apodization followed by a Lorentzian-to-Gaussian transformation was applied in both dimensions; forward linear prediction to twice the number of the original data points was employed in the indirect dimension followed by zero filling to twice the total number of points.

Numerical Simulations. Numerical simulations of the REDOR dephasing curves were performed using the *SPINEVOLUTION* program.[61] In the simulations, only the amide ^{15}N atoms and ^{13}C atoms were included. The coordinates of the ^{13}C and ^{15}N atoms in thioredoxin were obtained directly from the X-ray structure (PDB file 2trx.ent). To analyze the ^{15}N−^{13}C REDOR dephasing profiles of the amide ^{15}N spins in the U−^{13}C,^{15}N enriched fragment, the ^{13}C spins within 4 Å were selected. For the amide ^{15}N spins in the U−^{15}N labeled fragment and at the interface, the ^{13}C atoms within 6 Å (belonging to the U−^{13}C,^{15}N enriched fragment) were included in the simulations.

Results and Discussion

Control Experiments and Simulations. REDOR is an elegant technique for heteronuclear dipolar recoupling under MAS, by using a simple rotor-synchronous π pulses train.[46] REDOR is generally used for internuclear distance measurements. In this work, we employed REDOR for a different purpose: as an effective heteronuclear dephasing method to achieve complete and selective removal of the amide ^{15}N signals belonging exclusively to the 1–73(U−^{13}C,^{15}N) enriched thioredoxin fragment following the excitation of the ^{15}N signals from the entire protein. As detailed in the subsequent sections, the remaining ^{15}N magnetization is from the 74–108(U−^{15}N) fragment, and is employed to establish the intermolecular (through-interface) ^{15}N−^{13}C or intramolecular ^{15}N−^{1}H or ^{15}N−^{15}N correlations, for structural analysis of the interface and of the 74–108(U−^{15}N) fragment. To establish the experimental conditions necessary for the effective and selective dephasing of the desired signals and for the long-range magnetization transfer across the interface, we have executed a number of control experiments and numerical simulations discussed below.

1D ^{13}C-^{15}N REDOR Experiments and Simulations of REDOR Dephasing Curves in Intact and Reassembled Thioredoxin. For the backbone ^{15}N spins in 1–73(U−^{13}C,^{15}N) enriched fragment of thioredoxin, there are several ^{13}C spins that can contribute to the REDOR dephasing of the corresponding ^{15}N signals: generally the two C^{α} and C′ carbons directly bonded to the nitrogen (C−N distance of ∼1.4 Å), another two carbons within two bonds (C−N distance of ∼2.5 Å), and a number of carbon atoms separated by three or more bonds from the nitrogen (C−N distances between 4 and 7 Å). Carbon atoms within 4 Å are expected to have the largest contributions to the ^{13}C−^{15}N REDOR dephasing.

To establish the REDOR dephasing behavior, we have simulated the ^{15}N/^{13}C REDOR dephasing curves of the amide ^{15}N spins in thioredoxin using SPINEVOLUTION.[61] The atomic coordinates of the ^{15}N and ^{13}C spins in the simulations were taken directly from the X-ray structure of thioredoxin. ^{13}C−^{15}N spin pairs whose internuclear distances are within 4 Å were included in the simulations. Figure 3 depicts the simulated REDOR dephasing curves for V16, M35, and K57 residues of thioredoxin, which are located in an α-helix, a loop, and a β-strand, respectively.

As expected, due to the different ^{13}C−^{15}N dipolar coupling fields resulting from the distinct neighboring residue environ-

(59) Delaglio, F.; Grzesiek, S.; Vuister, G. W.; Zhu, G.; Pfeifer, J.; Bax, A. *J. Biomol. NMR* **1995**, *6*, 277–293.
(60) Goddard, T. D.; Kneller, D. G. *Sparky*;University of California, San Francisco.
(61) Veshtort, M.; Griffin, R. G. *J. Magn. Reson.* **2006**, *178*, 248–282.

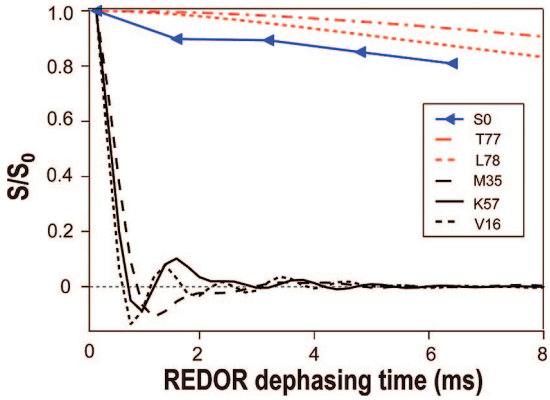

Figure 3. Simulated $^{15}N/^{13}C$ REDOR S/S_0 curves of amide ^{15}N spins in the 1–73(U-$^{15}N/^{13}C$)-labeled fragment (black), and in the 74–108(U$-^{15}N$)-labeled fragment at the intermolecular interface formed by antiparallel β-strands (red) of the 1–73(U$-^{13}C,^{15}N$)/74–108(U$-^{15}N$) thioredoxin reassembly. S/S_0 is the REDOR fraction. The Δ symbols do not represent a simulated S/S_0 curve but show the experimental T_2 decay of the reference intensity S_0 (blue curve).

ments and distinct conformations, the $^{13}C-^{15}N$ REDOR dephasing curves are slightly different for V16, M35, and K57. The ^{15}N S/S_0 curves decay rapidly to reach the minimum value during the first 0.8–1.2 ms of REDOR dephasing, and then oscillate around zero with decaying amplitude between 1 and 4 ms of dephasing time. After 4 ms, the residual intensity is generally smaller than 1–2% of the maximum value, with the complete dephasing accomplished after 6 ms. Faster dephasing is expected if additional carbon atoms within 4–7 Å are included in the simulations (which with the present computational resources is not feasible). According to these results, REDOR dephasing times of 4–6 ms are sufficient for complete removal of ^{15}N signals belonging to the (U$-^{13}C,^{15}N$) enriched fragment of the protein.

Indeed, the REDOR dephasing behavior predicted by the simulations is corroborated experimentally. In Figure 4, the following ^{15}N 1D spectra are illustrated for the U$-^{13}C,^{15}N$ enriched intact thioredoxin: (a) a reference spectrum where after the initial $^1H-^{15}N$ cross polarization a 6.4 ms T_2 decay was introduced, (b) a spectrum where after the initial $^1H-^{15}N$ cross polarization a 4.4 ms $^{13}C-^{15}N$ REDOR dephasing was incorporated; and (c) same as in spectrum b but with 6.4 ms REDOR dephasing. The overall envelope of the reference spectrum a is indistinguishable from the CPMAS spectrum with no relaxation decay (data not shown), albeit ca. 15–20% of the intensity is lost due to relaxation (see below). On the other hand, the REDOR spectra with both 4.4 and 6.4 ms dephasing exhibit no ^{15}N amide signals. We therefore conclude that the REDOR dephasing time of 4.4 ms is sufficient for complete removal of the ^{15}N signals in the U$-^{13}C$, ^{15}N-enriched protein. We additionally note that the amide nitrogen signals of the residues located on both ends of the polypeptide chain in thioredoxin, S1 and A108, are also cleanly dephased by REDOR, suggesting that the one- and two-bond dipolar couplings dominate the dephasing profile.

The same experiments were also carried out on the 1–73(U$-^{13}C,^{15}N$)/74–108(U$-^{15}N$) thioredoxin reassembly. Figure 4 depicts the following spectra of the 1–73(U$-^{13}C,^{15}N$)/74–108(U$-^{15}N$) reassembled sample: (d) a reference spectrum where after the initial $^1H-^{15}N$ cross polarization a 4.4 ms T_2 decay was introduced, and (e) a spectrum where after the initial $^1H-^{15}N$ cross polarization a 4.4 ms $^{13}C-^{15}N$ REDOR dephasing was incorporated. Similarly to the full-length intact thioredoxin sample, the reference spectrum in the presence of the T_2 decay was indistinguishable from the CPMAS spectrum. However, in the presence of the REDOR dephasing, many of the peaks disappear alleviating the spectral congestion. We note that the overall spectral envelope is distinctly different from the spectrum in the absence of the REDOR pulses, suggesting selective dephasing of the ^{15}N signals from the residues belonging to the 1–73(U$-^{13}C,^{15}N$) enriched fragment. While it is not possible to assign the remaining resonances to the specific residues on the basis of this 1D spectrum alone, the two-dimensional experiments detailed below confirm the expected selective dephasing of the (U$-^{13}C,^{15}N$)-enriched portion of the reassembly.

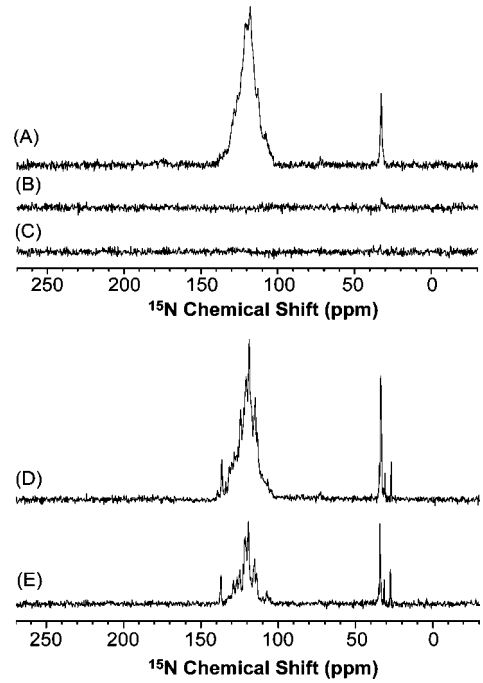

Figure 4. (Top) The $^{15}N/^{13}C$ REDOR spectra of U$-^{13}C,^{15}N$ labeled intact thioredoxin: (a) reference spectrum with the 6.4 ms T_2 decay and no REDOR dephasing; (b) with 4.4 ms REDOR dephasing; and (c) with 6.4 ms REDOR dephasing. Each FID was 256 scans, with the recycle delay of 2 s. (Bottom) The $^{15}N/^{13}C$ REDOR spectra of 1–73(U$-^{13}C,^{15}N$)/74–108(U$-^{15}N$) reassembled thioredoxin: (d) without REDOR dephasing; and (e) with 4.4 ms REDOR dephasing. These spectra were acquired with 852 scans and the recycle delay of 2 s.

As described above, we have observed the loss of ^{15}N signal intensity in the 74–108(U$-^{15}N$)-enriched fragment due to REDOR. To understand the origins of such intensity loss, we have conducted additional experiments. One possible factor leading to the loss of ^{15}N intensity is T_2 relaxation during REDOR. Indeed, introducing a T_2 relaxation delay after the CPMAS period resulted in a reduction of the signal intensity by an amount that expectedly depended on the duration of the delay. At 14.1 T, with the MAS rate of 10 kHz, and with the TPPM decoupling field strength of 100 kHz, we have observed that the ^{15}N signal intensity loss was ~15% and ~20% for 4.4 and 6.4 ms T_2 decay, respectively. The loss of intensity caused by the T_2 relaxation during REDOR depends on the magnetic field, MAS rate, and the ^1H decoupling field strength. With increasing spinning speed and ^1H decoupling field strength, the ^{15}N signal intensity loss is anticipated to be decreased significantly due to the longer T_2 of protein.

Another possible factor causing the loss of ^{15}N intensity in the U−^{15}N labeled fragment might be the ^{13}C/^{15}N REDOR dephasing from ^{13}C spins in the U−^{13}C,^{15}N enriched fragment and across the interface of the protein. This possible REDOR dephasing effect was estimated by simulations. In the X-ray structure, there are five and eight ^{13}C spins in the U−^{13}C,^{15}N fragment within the distance of 6 Å from the amide ^{15}N spins of T77 and L78 residues, respectively. Using these ^{13}C−^{15}N spin pairs, the corresponding REDOR dephasing curve was simulated. As shown in Figure 3, the loss of the amide ^{15}N signal intensity in T77 is ∼3% and 6%, while the corresponding loss for L78 is ∼10% and 16% with 4.4 and 6.4 ms dephasing time, respectively.

As demonstrated above, the REDOR experimental results are consistent with the simulations. Both simulations and experiments show that ^{13}C/^{15}N REDOR is an effective method to remove completely the backbone ^{15}N signals of the U-(^{13}C,^{15}N) enriched fragment in thioredoxin, which is expected to work equally well in any protein reassembly. The above results also demonstrate that despite the 10–30% possible intensity losses in the U−^{15}N fragment during the REDOR dephasing under moderate spinning and decoupling conditions, sufficient signal remains for the subsequent magnetization transfer steps. On the basis of the above results, for this work we have selected the 4.4 and 6.4 ms REDOR dephasing times for the PDSD−REDOR and HETCOR−REDOR/REDOR−PAINCP 2D experiments discussed below.

MAS Experiments for Structural Analysis of Differentially Enriched Protein Interfaces and Protein Assemblies. REDOR−PAINCP Spectroscopy. In this experiment, after the ^{13}C−^{15}N REDOR dephasing of the ^{15}N magnetization from the 1–73(U−^{13}C,^{15}N) fragment of reassembled thioredoxin, the ^{15}N magnetization from the 74–108(U−^{15}N) part of the protein is transferred to the aliphatic or ^{13}C′ spins across the interface, using PAINCP. The previous study[55] and our control PAINCP experiments on Met-Leu-Phe (MLF) tripeptide (see Supporting Information) suggest that PAINCP may be advantageous for establishing through-interface N−C contacts in thioredoxin reassembly owing to (i) the higher transfer efficiency for long-range N−C correlations compared with SPECIFIC-CP[62]; (ii) the effective suppression of one-bond correlations at long PAINCP mixing times. The second consideration is particularly important for the following reason. If a very small fraction of ^{15}N magnetization from the 1–73(U−^{13}C,^{15}N) fragment is not completely dephased by REDOR in the first part of the experiment, it will subsequently participate in the ^{15}N−^{13}C transfer, giving rise to the intramolecular one-bond ^{15}N−^{13}C correlations that will interfere with the long-range intermolecular cross peaks. As we have observed (data not shown), these one-bond transfers due to the residual magnetization are problematic if double cross polarization (DCP) under SPECIFIC-CP conditions[62] is employed for the ^{15}N−^{13}C transfer step, because the transfer efficiencies for one-bond correlations can be 5–10 fold higher compared with those for long-range correlations. On the other hand, if PAINCP is employed with 5–6 ms contact times, the long-range correlations have 50–100% transfer efficiency of that for one-bond correlations, as discussed in the Supporting Information and shown in Figure S1. In practice, we have observed that one-bond correlations are not present in the REDOR−PAINCP spectra of thioredoxin reassembly (Figure 5).

(62) Baldus, M.; Petkova, A. T.; Herzfeld, J.; Griffin, R. G. *Mol. Phys.* **1998**, *95*, 1197–1207.

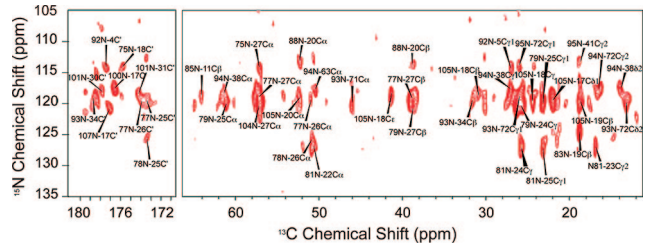

Figure 5. 2D REDOR−PAINCP spectra of the 1–73(U−^{13}C,^{15}N)/74–108(U−^{15}N) thioredoxin reassembly. The spectra were collected as 100 complex t_2 and 78 real t_1 points with 3000 scans. The spectral widths were 50 and 6 kHz in t_2 and t_1 dimensions, respectively. The recycle delay was 1.5 s.

The REDOR−PAINCP spectra of thioredoxin reassembly are shown in Figure 5. Two separate experiments were conducted with the ^{13}C frequency centered at 54 and 175 ppm for detection of aliphatic and carbonyl ^{13}C signals, respectively. In these two experiments, the rf field strengths on the ^{13}C and ^{15}N channels during the PAINCP period are 45 kHz, while the ^{1}H rf field strengths are 59 and 62.5 kHz for the detection of the aliphatic and carbonyl carbons, respectively. These were experimentally optimized to obtain the maximum intensity for the long-range correlations.

The REDOR−PAINCP spectra were assigned on the basis of the known ^{13}C and ^{15}N chemical shifts of the 1–73(^{13}C,^{15}N)/74–108(^{15}N) thioredoxin reassembly,[23] and on the basis of the ^{15}N chemical shifts of the 74–108(^{15}N) fragment obtained by a combination of PDSD−REDOR and HETCOR−REDOR spectra (see later). We note that there are two types of intermolecular interfaces in this reassembly which may give rise to long-range N−C cross peaks: (i) the interfaces formed by the two complementary fragments within a single molecule of reassembled thioredoxin, one formed by β2 and β4 strands (interface I), and another one formed by the α2 helix and the loop bridging the β5 sheet and α4 helix (interface II); and (ii) the interface formed by two molecules of reassembled thioredoxin (interface III). The N−C correlations in interfaces I and II arise from the N−C pairs of the complementary fragments within ∼7 Å, while the N−C correlations from interface III arise from the residues at the surface of two reassembled thioredoxin molecules. The resonance assignments and the corresponding N−C X-ray distances between residue pairs giving rise to cross peaks in the REDOR−PAINCP spectra are summarized in Table 1, and discussed briefly in the following.

Interface I formed by the two complementary 1–73(^{13}C,^{15}N) and 74–108(^{15}N) fragments of thioredoxin reassembly consists of two antiparallel β strands: β2 formed by residues 23–29, and β4 formed by residues 76–82.[48,49] Fifteen N−C contacts between the β2 and β4 strands were detected in the REDOR−PAINCP spectra. For example, several N−C correlations were observed between the amide nitrogen of F81 and the carbon atoms belonging to the residues in the 1–73(^{13}C,^{15}N) fragment: A22C$^{\alpha}$, I23C$^{\gamma}$, L24C$^{\gamma}$, and V25C$^{\gamma}$. Similarly, the amide nitrogen of L79 shows correlations to several carbon atoms of the β2 strand: V25C$^{\alpha}$, F27C$^{\alpha}$, L24C$^{\beta}$, and L24C$^{\gamma}$. We note that these correlations are also consistent with the results of REDOR−HETCOR spectra, in which the amide ^{1}H^{N} of F81 and L79 show strong C−H REDOR dephasing (see the REDOR−HETCOR spectra below). The correlations between amide nitrogens of several other residues, such as I75, T77, and L78, and aliphatic carbons of the residues in the β2 strand are also observed in the REDOR−PAINCP spectra (Figures 5,

Table 1. Summary of all Long-Range N−C Contacts Detected by the REDOR−PAINCP Spectra in Figure 5 [a]

residues	δ^{15}N (ppm)	residues	^{13}C type	δ^{13}C (ppm)	N−C distance (Å)
		Contacts within Interfaces I and II			
I75	114.6	F27	C^{α}	57.3	6.24
T77	119.4	F27	C^{α}	57.3	4.80
T77	119.4	D26	C^{α}	50.8	5.85
T77	119.4	D26	C′	173.9	5.63
T77	119.4	V25	C′	173.4	7.11
L78	125.8	D26	C^{α}	50.8	5.34
L78	125.8	V25	C′	173.4	5.47
L79	120.3	L24	C^{γ}	25.8	5.41
L79	120.3	V25	C^{α}	61.2	4.59
L79	120.3	V25	$C^{\gamma 1}$	23.0	5.61
L79	120.3	F27	C^{β}	39.1	6.71
F81	127.6	A22	C^{α}	51.0	5.74
F81	127.6	*I*23	$C^{\gamma 2}$	16.6	4.67
F81	127.6	L24	C^{γ}	25.8	6.9
F81	127.6	V25	$C^{\gamma 1}$	23.0	5.9
A93	119.7	P34	C^{β}	31.4	4.9
A93	119.7	P34	C′	179.6	5.94
L94	118.0	I38	C^{α}	61.5	6.41
L94	118.0	I38	$C^{\gamma 1}$	27.0	3.96
L94	118.0	I38	$C^{\gamma 2}$	13.8	5.84
		Contacts within Interface III			
I75	114.6	K18	C′	175.5	
N83	124	A19	C^{β}	18.8	
E85	118.3	S11	C^{β}	64.0	
A88	113.1	A20	C^{α}	52.4	
A88	113.1	A20	C^{β}	38.7	
G92	114.4	I4	C′	177.2	
G92	114.4	I5	$C^{\gamma 2}$	26.6	
A93	119.7	I72	$C^{\gamma 1}$	25.9	
A93	119.7	I72	$C^{\delta 1}$	13.1	
L94	118.0	N63	C^{α}	50.6	
L94	118.0	I72	$C^{\delta 2}$	15.9	
K100	117.8	A19	C′	176.4	
E101	118.1	E30	C’	177.4	
E101	118.1	W31	C’	174.1	
D104	120.2	L17	C^{α}	57.0	
A105	120.3	L17	$C^{\delta 1}$	22.1	
A105	120.3	K18	C^{ϵ}	41.4	
A105	120.3	K18	C^{β}	30.5	
A105	120.3	A19	C^{β}	18.8	
A105	120.3	A20	C^{α}	52.4	

[a] The first part of this table is N−C contacts within interfaces I and II formed by the two complementary 1–73(^{13}C,^{15}N) and 74–108(^{15}N) fragments of thioredoxin reassembly. The N−C internuclear distances were obtained from X-ray crystal structure (PDB file 2trx.ent). The second part is the N−C contacts within interface III formed by two different molecules of reassembled thioredoxin.

6, and Table S1 of the Supporting Information). Interface II is formed by the residues lining the α2 helix in the 1–73(^{13}C,^{15}N) fragment and the loop bridging the β5 sheet and the α4 helix in the 74–108(^{15}N) fragment. For instance, cross peaks were observed between the amide ^{15}N atom of L94 and the C′, C^{α}, C^{γ}, and $C^{\delta 2}$ atoms of I38. Figure 6 illustrates the long-range contacts belonging to interfaces I and II and detected in REDOR−PAINCP spectra.

The correlations between the residues of interface III formed by two different molecules of reassembled thioredoxin were also observed in the REDOR−PAINCP experiments, as illustrated in Figure 5 and Table S1 of the Supporting Information. For example, A93 and L94 located in the β5 strand, show correlations with I72 located in the loop joining the α3 helix and the β4 strand. Similarly, D104 and A105 of the α4 helix exhibit contacts with K18, A19, and A20 of the loop joining the α1 helix and the β2 strand.

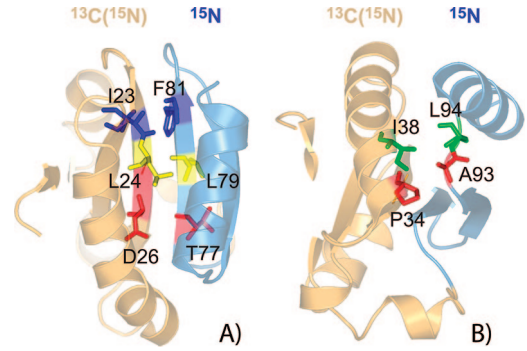

Figure 6. The intermolecular correlations between the residues of the interfaces formed by the 1–73(U−^{13}C,^{15}N) and 74–108(U−^{15}N) fragments in thioredoxin reassembly, which were detected in the REDOR−PAINCP experiment: (A) correlations observed within interface I; (B) correlations observed within interface II.

It is important to note that the cross peak intensity in the REDOR−PAINCP spectra is determined by the combined effect of the H−N CP transfer efficiency, ^{15}N T_2 decay, and ^{15}N−^{13}C dephasing during REDOR and PAINCP. About half of pairs of the residues that are in contact at the interfaces I and II were detected by REDOR−PAINCP spectra, compared with the X-ray structure. The signals belonging to the residues with short T_2 times and increased molecular mobility, or those where the PAINCP transfer efficiencies are low, are generally weak or missing. One example is P76, the correlations to which are missing in REDOR−PAINCP spectra. The absence of protons directly bonded to the amide nitrogen in this proline residue results in the low PAINCP transfer efficiency. The main limitation under our experimental conditions (moderate magnetic field strength, moderate MAS frequency, and moderate decoupling fields) is relatively low transfer efficiency for the long-range correlations established via PAINCP. The transfer efficiency of the long-range N−C PAINCP correlations can be improved significantly at higher magnetic fields or higher MAS frequencies (>20 kHz) and/or higher decoupling fields, as demonstrated by the results of Lewandowski et al. at 17.6 T[55] and by our PAINCP 2D experiments on MLF peptide conducted at 14.1 T (see Supporting Information). The enhanced PAINCP performance is anticipated to result in a larger number of through-interface cross peaks in the REDOR−PAINCP spectra.

PDSD−REDOR and HETCOR−REDOR Spectroscopy. In the previous study, we have reported resonance assignments of the ^{13}C and ^{15}N chemical shifts of the 1–73(U−^{13}C,^{15}N) enriched fragment of the 1–73(U−^{13}C,^{15}N)/74–108(U−^{15}N) thioredoxin reassembly.[23] In this work, we introduce PDSD−REDOR and HETCOR−REDOR experiments for assignments of the ^{15}N and ^{1}H chemical shifts of the backbone amide residues in the 74–108(U−^{15}N) enriched fragment of the protein. To obtain ^{15}N−^{15}N and ^{1}H−^{15}N correlations arising exclusively from the 74–108(U−^{15}N) enriched part of the reassembly, we have introduced a ^{13}C−^{15}N REDOR dephasing period into the ^{15}N PDSD and ^{1}H−^{15}N FSLG−HETCOR sequences. As illustrated by the control experiments, REDOR dephasing is expected to remove selectively and completely the backbone ^{15}N signals from the 1–73(U−^{13}C,^{15}N) fragment, leaving only the 35 backbone ^{15}N signals (as well as the side chain ^{15}N signals) of the 74–108(U−^{15}N) C-terminal part. Indeed, as shown in Figure 7 (b, c, e, and f), the cross peaks corresponding to the amide nitrogens of the 1–73(U−^{13}C,^{15}N) fragment are completely removed with the REDOR period. Even though as discussed above, introduction of REDOR dephasing results in

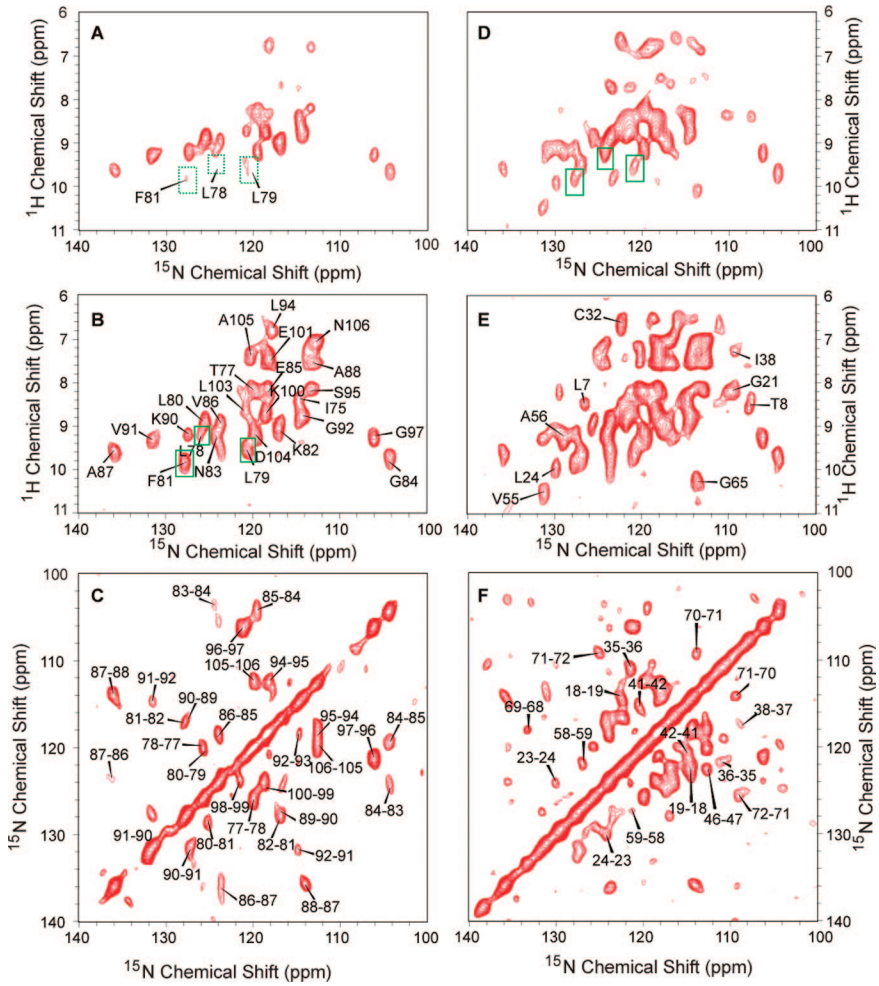

Figure 7. 2D REDOR−HETCOR (A), HETCOR−REDOR (B), PDSD−REDOR (C) and the corresponding reference spectra D, E, and F of the 1–73(U−^{13}C,^{15}N)/74–108(U−^{15}N) thioredoxin reassembly. In the reference spectra D−F, the ^{15}N/^{13}C REDOR dephasing period is replaced by a delay to ensure the identical T_2 relaxation behavior; 3.2 ms ^{1}H/^{13}C, 6.4 ms, and 4.4 ms ^{15}N/^{13}C REDOR dephasing times were used in the REDOR−HETCOR, HETCOR−REDOR, and PDSD−REDOR experiments, respectively. Spectra A and D were acquired with 500 complex t_2 and 80 real t_1 points with 720 scans; the spectral widths were 20 and 13.2 kHz in the t_2 and t_1 dimensions, respectively. Spectra B and E were acquired with 500 complex t_2 and 128 real t_1 points, and 256 scans; the spectral widths were 20 and 20.1 kHz in the t_2 and t_1 dimensions, respectively. Spectrum C was collected with 625 complex t_2 and 64 real t_1 points, and 720 scans; the spectral widths were 20 and 6 kHz in the t_2 and t_1 dimensions, respectively. Spectrum F was acquired with 625 complex t_2 and 128 real t_1 points, and 120 scans; the spectral widths were the same as in spectrum C. The recycle delay was 1.5 s in all spectra.

15–20% intensity loss of the remaining signals from the 74–108(U−^{15}N) fragment, high quality spectra could be obtained. Most importantly, the alleviation of the spectral congestion allowed for the resonance assignments of the ^{15}N and ^{1}H signals in the 2D NN and NH correlation spectra.

The N−N PDSD mixing time utilized in the REDOR−PDSD experiments was 4 s. Under these conditions, almost all of the cross-peaks are from the sequential N_iN_{i-1} correlations, and the cross peak intensities are 10–30% of the corresponding diagonal signals. The cross peaks from N_iN_{i-2} correlations are too weak to be detected. The amide ^{15}N chemical shifts of residues 74–108 in 1–73(U−^{13}C, ^{15}N)/74–108(U−^{15}N) thiredoxin reassembly shown in PDSD−REDOR spectra are very similar to those of the 1–73(U−^{15}N)/74–108(U−^{13}C,^{15}N) thioredoxin complex. The amide ^{15}N chemical shifts of residues 74–108 in the 1–73(U−^{15}N)/74–108(U−^{13}C,^{15}N) thioredoxin were assigned in our previous study.[22] Almost all of the cross peaks for the 1–73(U−^{13}C,^{15}N)/74–108(U−^{15}N) thioredoxin reassembly in this work could be assigned on the basis of these previous assignments. Cross peaks from almost all residues were present in the spectra, with the following exceptions: G74, I75, P76, and A108. The cross peak corresponding to P76 is missing likely because there is no directly attached proton, and the efficiency of the magnetization transfer is low. This was also previously observed for proline residues by Oschkinat et al.[63] G74 and I75 residues are located at the beginning of the C-terminal fragment and at interface I, and their nitrogen signals are likely dephased during the REDOR period due to the close proximity of the carbons from I72 and R73 in the 1–73(U−^{13}C,^{15}N) enriched fragment.

In the N−H FSLG-based HETCOR and HETCOR−REDOR experiments, a flat CP with the contact time of 170 μs was employed to establish the correlations between the amide ^{1}H and ^{15}N spins. Under these conditions, only the correlations corresponding to the directly bonded NH pairs are observed, and ca. 70% of the signal intensity of the ^{1}H/^{15}N CP is retained. The ^{1}H homonuclear FSLG decoupling during the t_1 evolution yields the ^{1}H line width of 0.4–0.6 ppm in the indirect dimension. This resolution permits the unambiguous assignment of the majority of the ^{1}H and ^{15}N chemical shifts in the

(63) van Rossum, B. J.; Castellani, F.; Pauli, J.; Rehbein, K.; Hollander, J.; de Groot, H. J. M.; Oschkinat, H. *J. Biomol. NMR* **2003**, *25*, 217–223.

HETCOR−REDOR spectra. The ambiguity for several residues with similar ^{15}N chemical shifts but distinct ^{1}H shift was resolved by using the ^{1}H solution chemical shifts of the corresponding residues, which were obtained from the 2D HN HSQC and 3D HNCA spectra of 1–73(U−^{13}C,^{15}N)/74–108(U−^{15}N) reassembled thioredoxin (experimental conditions are given in the Supporting Information). We note that in the HETCOR−-REDOR spectra, the signals from P76 and G74 were missing, similar to the PDSD−HETCOR spectra discussed above.

On the basis of the N−N PDSD−REDOR and N−H HETCOR−REDOR spectra, we have assigned unambiguously 32 (of 35) amide ^{15}N signals in the 74–108(U−^{15}N) enriched fragment.

REDOR−HETCOR Spectroscopy. The ^{13}C−^{1}H^{N} dipolar interaction is 10 times stronger than the ^{13}C−^{15}N coupling for the identical internuclear distance because $\gamma(^{1}\mathrm{H})/\gamma(^{15}\mathrm{N}) \approx 10$. The large C−H dipolar interaction permits measurement of long-range distances using ^{1}H/^{13}C REDOR, as has been demonstrated previously.[58] Alternatively, ^{1}H−^{13}C REDOR dephasing in conjunction with ^{15}N detection, can be applied for detection of long-range ^{13}C···(^{1}H^{N})-^{15}N correlations.

The pulse sequence for the two-dimensional NH REDOR−HETCOR experiment is based on the modified one-dimensional N-detected REDOR experiment designed by Schmidt-Rohr and Hong for measurement of the ^{13}C−^{1}H^{N} distances.[58] As shown in Figure 2, the proton magnetization is first dephased by ^{1}H/^{13}C REDOR, followed by a ^{1}H chemical shift evolution, a subsequent ^{1}H−^{15}N magnetization transfer by a flat CP with a short contact time, and a detection of the ^{15}N signal during t_2. During the REDOR and the ^{1}H chemical shift evolution in the indirect dimension, the ^{1}H−^{1}H homonuclear dipolar coupling is suppressed by FSLG decoupling, which was implemented by ramping the phase of the ^{1}H RF pulses while keeping the carrier frequency constant. It should be noted that in the regime of high MAS frequency, FSLG is a more effective homonuclear decoupling method than the MREV-8 technique employed in the previous work for slower MAS conditions.[58]

With the 3.2 ms ^{1}H−^{13}C REDOR dephasing, the ^{1}H^{N} signals belonging to the 1–73(U−^{13}C,^{15}N) enriched fragment are eliminated completely, as illustrated in Figure 7. The ^{1}H^{N} signals in the 74–108(U−^{15}N) fragment exhibit different REDOR dephasing behavior. Those signals that are away from the 1–73(U−^{13}C,^{15}N)/74–108(U−^{15}N) interface experience only weak dephasing from the natural abundance ^{13}C spins, resulting in a small fraction of intensity lost. The ^{1}H^{N} signals corresponding to the residues at the interface of the reassembled thioredoxin, undergo strong dephasing by the ^{13}C signals from the 1–73(U−^{13}C,^{15}N) enriched fragment, resulting in the disappearance of the corresponding peaks or in a significant intensity loss. For example, the ^{1}H^{N}-^{15}N cross peaks which belong to the interface residues L78, L79, and F81, and which are present in the control REDOR−HETCOR experiment (where the REDOR dephasing pulses are replaced by the delay to account for the T_2 relaxation during REDOR) as well as in the HETCOR−REDOR experiment, are missing in the REDOR−HETCOR spectra. For cross peaks belonging to other residues at the interface, such as T77, we observed a significant intensity loss in the REDOR−HETCOR spectra compared to the control experiment and to the HETCOR−REDOR experiment. These results indicate that REDOR−HETCOR is a useful experiment for identification of the residues at the interface of reassembled thioredoxin.

It is important to note that under our experimental conditions we observed considerable (ca. 60–70%) loss of the ^{1}H^{N} intensity during FSLG, which is due to the fast ^{1}H T_2 relaxation in thioredoxin reassembly under our experimental conditions. As shown in Figure 7, in the control REDOR−HETCOR spectra where the REDOR dephasing pulses were replaced by the 3.2 ms delay, a number of peaks were missing in the spectrum due to T_2 decay (e.g., E85, A88, S95). Nevertheless, the remaining ^{1}H signal intensity is still sufficient to produce high-quality REDOR−HETCOR spectra of thioredoxin (Figure 7).

We also note that for some peaks it is difficult to measure the cross peak intensity in the 2D REDOR−HETCOR spectra because of substantial signal overlap. In reassembled thioredoxin, this overlap is most pronounced for the ^{15}N chemical shift range between 119 and 130 ppm, where a number of nitrogen signals from both fragments appear. REDOR dephasing results in a complete removal of the signals belonging to the 1–73(U−^{13}C,^{15}N) fragment, and for the overlapping regions it is impossible to determine unambiguously whether the loss of intensity in some of the cross peaks is due to the REDOR dephasing of the interface residues from the 74–108(U−^{15}N) fragment by the ^{13}C spins from the 1–73(U−^{13}C,^{15}N) fragment. Increasing the dimensionality of the REDOR−HETCOR experiment is one strategy expected to alleviate the assignment problem for the congested regions of the spectra. An alternative (and more information-rich) approach is the REDOR−PAINCP spectroscopy introduced above.

^{13}C,^{15}N/^{15}N Differential Isotopic Enrichment for Studies of Protein–Protein Interactions by MAS NMR Spectroscopy. In our previous studies, we have shown the simplification of resonance assignments of the individual fragments in thioredoxin reassemblies using the (^{13}C,^{15}N/^{15}N) differential isotopic enrichment approach.[22,23] This type of enrichment does not require any special expression systems or bacteria growth procedures, and can be employed for many proteins expressed in *E.coli*. In this report, we take this initial work to the next level and introduce a general approach for studies of protein–protein interactions by MAS NMR spectroscopy, which is based on a combined set of solid-state NMR experiments for analysis of protein interfaces and resonance assignments of the individual interacting proteins in the (^{13}C,^{15}N/^{15}N) differentially enriched assemblies. This approach is advantageous because it permits the assignments of the ^{13}C,^{15}N resonances of the U−^{13}C,^{15}N enriched partner and of the ^{1}H, ^{15}N resonances of the U−^{15}N enriched part, as well as the structural analysis of the interface formed by the two interacting proteins. In more general applications to structural analysis of protein assemblies formed by two interacting proteins, a single sample differentially enriched following the (^{13}C,^{15}N/^{15}N) protocol will be sufficient for the resonance assignments and complete structural characterization of the ^{13}C,^{15}N-labeled protein and for identifying its interaction interface with the binding partner, while a pair of samples differentially enriched in a complementary way will permit full structural analysis of both the interacting proteins and the intermolecular interface.

We have also demonstrated that ^{13}C/^{15}N REDOR is an effective technique to completely remove the ^{15}N signals in the U−^{13}C,^{15}N enriched proteins, and we envision that this will be a useful building block for designing MAS experiments for structural analysis of biomolecular protein assemblies with (^{13}C,^{15}N/^{15}N) differential enrichment. The (^{13}C,^{15}N/^{15}N) differential enrichment scheme can be expanded to (^{13}C,^{15}N/^{2}H,^{15}N) enrichment, where the introduction of ^{2}H is expected

to lead to higher resolution in the $^{1}H-^{15}N$ MAS spectra of the ^{2}H, ^{15}N enriched partner in the assembly. In conjunction with high MAS frequencies (40 kHz or higher), significant improvement of the ^{1}H resolution was demonstrated by recent studies.[64,65] In addition, using sparse ^{13}C labeling in the (^{13}C,^{15}N)-enriched fragment, for example following the 1,3- and 2-^{13}C enrichment protocol[66] the resolution and sensitivity of the ^{13}C dimension can be enhanced because of the reduction of the resonance overlap and narrowing of the linewidths due to the removal of the $^{13}C-^{13}C$ J coupling.[43]

The PDSD−REDOR, HETCOR−REDOR, and REDOR−PAINCP experiments reported here were conducted at moderate magnetic field (14.1 T), moderate MAS frequencies, and moderate decoupling field strengths. The performance of these pulse sequences is expected to improve at higher magnetic fields and under fast MAS. Under those conditions, higher intensities will permit the introduction of the third chemical shift dimension to the 2D sequences presented in this study, and we anticipate that protein assemblies considerably larger than thioredoxin will be amenable to detailed structural studies using these experiments. We anticipate that the experiments introduced in this work will be especially useful in complex protein assemblies in noncrystalline and insoluble environments that are difficult to be studied by other structural methods.

Conclusions

We introduced a family of heteronuclear two-dimensional MAS NMR correlation experiments for structural studies of protein interfaces in differentially (^{13}C,^{15}N/^{15}N) isotopically enriched protein assemblies. The $^{15}N-^{13}C$ REDOR−PAINCP experiment yields long-range N−C correlations arising from the residues at the interfaces formed by the two complementary fragments in a single molecule and at the interface formed by two molecules of reassembled thioredoxin. $^{15}N-^{15}N$ PDSD−REDOR and $^{1}H-^{15}N$ HETCOR−REDOR experiments yield correlations corresponding to the U−^{15}N enriched fragment of the reassembly, and permit its ^{15}N and ^{1}H chemical shift assignments. The $^{1}H-(^{13}C)-^{15}N$ REDOR−HETCOR experiment additionally highlights the residues at the interfaces formed by the two complementary fragments in a single molecule of reassembled thioredoxin. Our results suggest that the experimental protocols introduced in this study will be applicable to studies of protein–protein interactions in a broad range of systems.

Acknowledgment. The authors thank Marcela Cataldi and Dabeiba Marulanda for the preparation of the thioredoxin samples, and Sivakumar Paramasivam for acquiring the solution NMR spectra. T.P. and J.Y. thank Alexander J. Vega for useful discussions. This project was supported by the National Institutes of Health (NIH Grant No. P20 RR-015588 from the National Center for Research Resources) and by the National Science Foundation (NSF-CAREER CHE-0237612). M.L.T. is supported by the National Science Foundation (MCB-0517592) award and the National Institutes of Health (NIH Grant No. 5G12RR03060 from the National Center for Research Resources) grant to the 600 MHz NMR spectrometer at CCNY. M.L.T. is a member of the New York Structural Biology Center (NYSBC) supported by the National Institutes of Health (GM66354).

Supporting Information Available: Complete phase cycles for pulse sequences; control PAINCP experiments of MLF; solid-state ^{1}H and ^{15}N chemical shifts of 1–73(U−^{13}C,^{15}N)/74–108(U−^{15}N) reassembled thioredoxin; experimental conditions for solution NMR measurements. This material is available free of charge via the Internet at http://pubs.acs.org.

JA711304E

(64) Chevelkov, V.; Rehbein, K.; Diehl, A.; Reif, B. *Angew. Chem., Int. Ed.* **2006**, *45*, 3878–3881.
(65) Zhou, D. H.; Shah, G.; Cormos, M.; Mullen, C.; Sandoz, D.; Rienstra, C. M. *J. Am. Chem. Soc.* **2007**, *129*, 11791–11801.
(66) LeMaster, D. M.; Kushlan, D. M. *J. Am. Chem. Soc.* **1996**, *118*, 9255–9264.
(67) Laskowski, R. A.; Hutchinson, E. G.; Michie, A. D.; Wallace, A. C.; Jones, M. L.; Thornton, J. M. *Trends Biochem. Sci.* **1997**, *22*, 488–490.
(68) Katti, S. K.; LeMaster, D. M.; Eklund, H. *J. Mol. Biol.* **1990**, *212*, 167–184.
(69) DeLano, W. L. *Pymol*; DeLano Scientific, LLC: San Carols, CA, 2003.